Environ Earth Sci (2011) 63:97–107
DOI 10.1007/s12665-010-0672-6

ORIGINAL ARTICLE

Sensible and latent heat flux response to diurnal variation in soil surface temperature and moisture under different freeze/thaw soil conditions in the seasonal frozen soil region of the central Tibetan Plateau

Donglin Guo · Meixue Yang · Huijun Wang

Received: 9 July 2009 / Accepted: 6 July 2010 / Published online: 24 July 2010

Abstract The relationship between sensible and latent heat flux and diurnal variation in soil surface temperature and moisture under four freeze/thaw soil conditions was investigated using observed soil temperature and moisture and simulated sensible and latent heat flux. The diurnal range of latent heat flux had a similar temporal change pattern as that of unfrozen soil water at depths of 0–3 cm during the freezing stage. Also, there was a better relationship with the diurnal range of unfrozen soil water at depths of 3–6 cm during the thawing stage. Diurnal variation in latent heat flux was significant and depended mostly on solar radiation during the completely thawed stage. However, while diurnal variation in solar radiation during the completely frozen stage was significant, for latent heat flux it was quite weak due to low unfrozen soil water content. Thus, diurnal variation in latent heat flux depended mostly on unfrozen soil water content during this stage. During the freezing and thawing stages, diurnal variation in latent heat flux was also significant and depended mostly on diurnal variation in unfrozen soil water content. However, the impacts of air temperature change from solar radiation on latent heat flux could not be ignored.

D. Guo · H. Wang
Nansen-Zhu International Research Center,
Institute of Atmospheric Physics, Chinese Academy of Sciences,
Beijing 100029, China

D. Guo · M. Yang (✉)
State Key Laboratory of Cryospheric Sciences, Cold and Arid Regions Environmental and Engineering Research Institute,
Chinese Academy of Sciences, Lanzhou 730000, China
e-mail: mxyang@lzb.ac.cn

D. Guo
Graduate University of the Chinese Academy of Sciences,
Beijing 100049, China

Keywords Tibetan Plateau · Freeze/thaw · Soil water · Latent heat flux

Introduction

The Tibetan Plateau averages more than 4,000 m in elevation and is the highest and most extensive plateau in the world. It exerts a significant influence on general circulation (Wu and Chen 1985) and the progress of the Asian monsoon system through its anomalous mid-tropospheric heat source for southwestern Asia during summer (Ye and Gao 1979; Yanai et al. 1992; Wu and Zhang 1998; Ueda and Yasunari 1998; Duan and Wu 2005). The energy and water cycles over the Tibetan Plateau are arguably of heightened importance due to their far-reaching impacts across Asia, the northern hemisphere, and the globe. The sensible and latent heat fluxes released over the Tibetan Plateau not only strongly affect global circulation patterns (Webster 1987), but also show good correlation with the onset of the summer monsoon (Tanaka et al. 2001).

Land surface characteristics on the Tibetan Plateau are multifold and complex. Permafrost and seasonal frozen soil are extensively developed on the Plateau. Seasonally freeze/thaw processes of the land surface and their spatial distribution lead to spatiotemporal variations in surface wetness and to variations in the surface heat balance.

Diurnal freeze/thaw cycles of the land surface result in frequent phase transitions of soil water. These not only significantly influence the thermal condition of the soil, but also the energy/water exchanges between the land surface and atmosphere (Li et al. 2002) due to unequal thermal conductivities (ice: 2.2 W m^{-1} K^{-1}; water: 0.57 W m^{-1} K^{-1}) and capacities (ice: 1.9 MJ m^{-3} K^{-1}; water: 4.2 MJ m^{-3} K^{-1}). To quantify these influences is very important in order to

understand the energy and water cycle processes and their effects on the Asian monsoon system. However, limitations in data resolution (temporal and spatial) makes it difficult to quantify the diurnal freeze/thaw cycles of the soil surface layer and their impact on the interaction processes between the land surface and atmosphere.

In order to get to the bottom of the mechanisms of the Tibetan Plateau's impact on the Asian monsoon system, the Global Energy and Water Cycle Experiment/Asian Monsoon Experiment on the Tibetan Plateau (GAME-Tibet, 1996–2000), as well as the Coordinated Enhanced Observing Period/Asia–Australia Monsoon Project on the Tibetan Plateau (CAMP-Tibet, 2001–2005) were conducted by a joint Chinese–Japanese field team. The data collected during these projects have been used by many studies investigating the interaction between the land surface and atmosphere (Yang et al. 1999a, b, 2003, 2007; Ma et al. 2004, 2006; Ma et al. 2005; Ma and Ma 2006; Tanaka et al. 2001; Gao et al. 2004; Cheng et al. 2008; Guo et al. 2009a, b). Diurnal variation in sensible and latent heat flux, soil temperature, and soil moisture in different seasons has also been reported (Yu et al. 2004; Ma et al. 2005, 2006; Yang et al. 1999a, b, 2003, 2007; Zhao et al. 2007). However, few studies have focused on the relationship between sensible and latent heat flux and diurnal variation in soil surface temperature and moisture over the Tibetan Plateau.

The objectives of this paper, therefore, are to evaluate quantitatively this relationship during four freeze/thaw stages using observed soil temperature and moisture from the CAMP-Tibet project, and simulated sensible and latent heat fluxes based on the Simultaneous Heat and Water model.

Data and methods

Field measurement data

Site "BJ" (31.37°N, 91.90°E; 4,509 m) is an observational station of the CAMP-Tibet project. It is located in a relatively large open space, covering an area of approximately 30 × 50 km on flat Naqu grassland in a seasonal soil frost region of the central Tibetan Plateau (Fig. 1). Soil at this site is predominantly sandy silt loam with small and scattered pebbles. Vegetation cover is comprised of short grasses with a canopy height <5 cm and leaf area index <0.5 during the peak growth stage in late May to mid September (Gao et al. 2004).

General observation elements of the BJ site are shown in Table 1. The measurements of sensible and latent heat flux during November 27 2002–December 18 2002 and May 28 2003–Jun 20 2003 were derived from http://data.eol.ucar.edu/ (visited on January 1 2010). Data flagged B (bad) or D (dubious) were eliminated. Soil temperature and moisture at different depths during August 23 2002–May 23 2003 were observed to investigate the diurnal freeze/thaw cycles of surface layer soil. At the BJ site, there were 12 platinum temperature probes installed, which were positioned at 0, 0.5, 1, 2, 3, 4, 5, 6, 7, 8, 9, and 20 cm. In addition, there were four time-domain reflectometers installed at depths of between 0–3, 3–6, 6–9, and 18.5–21.5 cm for monitoring soil water content. The water content observed by the time-domain reflectometers denoted the unfrozen water content. All the probes were connected with two dataloggers, with data recorded at 30 min intervals.

Methods

Four soil freeze/thaw stages were defined without consideration of the effect of salinity on the soil freezing point. These stages were (1) the completely thawed stage (daily minimum soil temperature is >0°C); (2) the completely frozen stage (daily maximum soil temperature is <0°C); (3) the freezing stage (soil profile in the process of freezing); and (4) the thawing stage (soil profile in the process of thawing). The ground diurnal freeze/thaw cycles were judged to have occurred when the daily maximum soil temperature was >0°C but the daily minimum soil temperature was <0°C, a pattern existing on each day of the freezing and thawing stages. To avoid the potential impact of random weather processes on the movement from one soil freeze/thaw stage to the next, the occurrence of three consecutive days meeting a chosen set of criteria was used as the indicator of the transition, and the first day of these 3 days was recorded as the start date of the next freeze/thaw stage. Based on this assumption, four freeze/thaw stages at a depth of 2 cm were identified (Table 2).

Sensible and latent heat fluxes are not only affected by soil temperature and moisture, but also by changes in elements of the weather (e.g. snowfall, wind speed, air temperature and solar radiation). In order to analyze the response of sensible and latent heat fluxes to diurnal variation in soil surface temperature and moisture only, two continuous clear days from four freeze/thaw stages were chosen as a case study. Meanwhile, the input forcing data of the model were adjusted to remove the impact of changes in the weather on sensible and latent heat fluxes.

Model and parameter settings

The Simultaneous Heat and Water (SHAW) model was developed by Flerchinger et al. (1996), Flerchinger and Saxton (1989) and Flerchinger and Pierson (1991). The physical system of the SHAW model consists of a vertical,

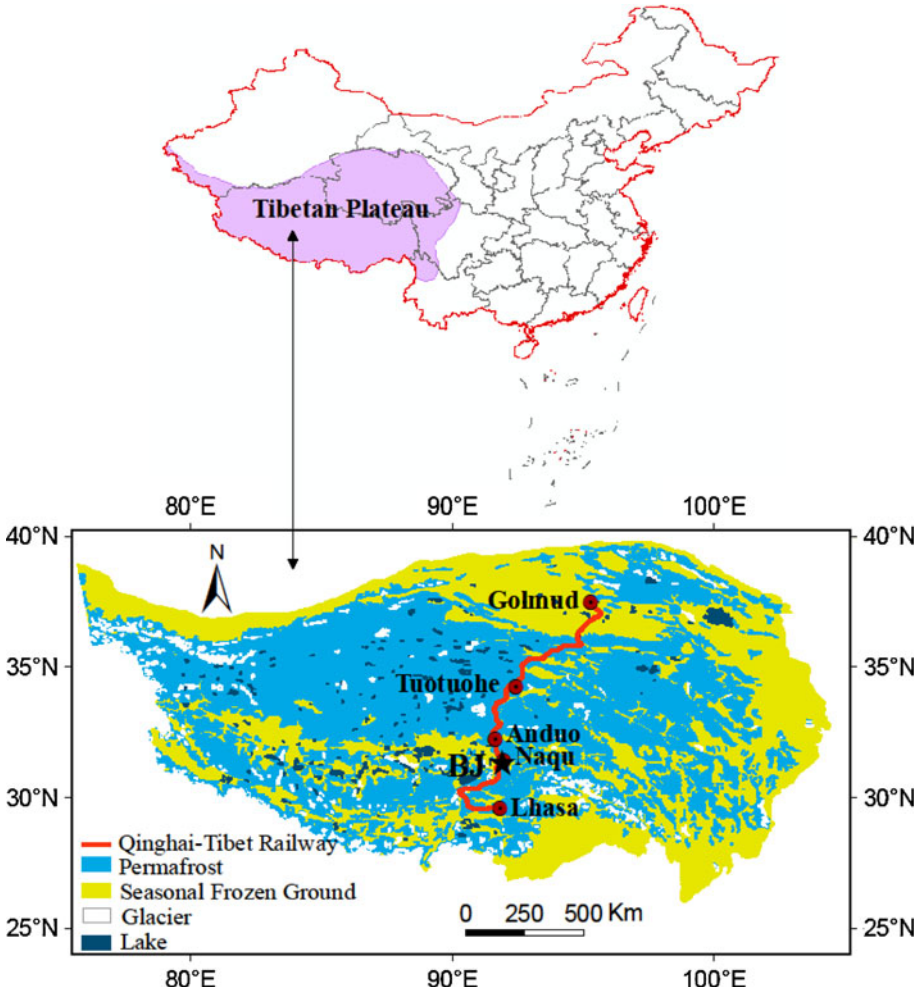

Fig. 1 Geographic location of site BJ

Table 1 Observation elements at site BJ

Observation elements	Height (m)
Wind speed* (m s^{-1})	10, 5, 1
Wind direction (°)	10
Air temperature* (°C)	8.2, 1
Specific humidity* (%)	8.2, 1
Atmospheric pressure (hPa)	Ground
Precipitation* (mm)	Ground
Radiation* (W m^{-2}) (DSR, DLR, USR, ULR)	
Soil heat flux* (W m^{-2})	0.1, 0.2
Soil temperature* (°C)	0.04, 0.2, 0.4, 0.6, 0.8, 1.0, 1.3,1.6, 2, 2.5
Soil moisture* (m^3 m^{-3})	0.04, 0.2, 0.6, 1.0, 1.6, 2.1

one-dimensional profile extending from the vegetation canopy, snow, residue, or soil surface to a specified soil depth. A layered system is established through the plant canopy, snow, residue, and soil, and each layer is represented by an individual node. Energy, moisture, and solute fluxes are computed between nodes for each time step. Balance equations for each node are written in implicit finite-different form and solved using an iterative Newton–Raphson technique. Unique features of the model include the simultaneous solution of heat, water, and solute fluxes, as well as detailed provisions for soil freezing and thawing. Heat and water fluxes into the system are defined by diurnal or hourly weather conditions (air temperature, wind speed, humidity, solar radiation, and precipitation) above the upper boundary and soil conditions at the lower boundary. The model not only considers the impact of unfrozen water, ice and vapor transfer on the water and heat balance, but also the latent heat flux generated when soil undergoes freezing or thawing. Soil volumetric water content is expressed as a function of soil matric potential. Additionally, the freezing temperature of water is adjusted so as to simulate accurately the various freeze/thaw processes in the soil.

The core theory of the SHAW model is the surface energy balance, which may be written as

Table 2 Starting dates of the four soil freeze/thaw stages during 2002–2003 (month-day)

Depth (cm)	Start date of the freezing stage	Start date of the completely frozen stage	Start date of the thawing stage	Start date of the completely thawed stage
0.5	10.3	12.31	1.25	
2	10.3	12.31	1.25	5.14
3	10.5	12.14	2.1	4.28
4	10.11	12.14	2.17	4.28
5	10.11	12.14	2.17	4.28
6	10.11	11.14	3.1	4.28
7	10.11	11.14	3.1	4.28
8	10.22	11.14	3.2	4.20
9	10.22	11.14	3.2	4.20
20	10.22	11.14	3.27	4.19

$$R_n + H + L_vE + G = 0, \quad (1)$$

where R_n is net radiation (W m^{-2}), H is sensible heat flux (W m^{-2}), L_vE is latent heat flux (W m^{-2}), G is soil or ground heat flux (W m^{-2}), L_v is latent heat of evaporation (J kg^{-1}), and E is total evapotranspiration from the soil surface and plant canopy (kg m^{-2} s^{-1}). Net radiation is determined by the transmission of solar radiation and long-wave radiation in the layers of the plant canopy, residue, and soil. Soil heat flux is calculated with Eq. 1, which satisfies the whole balance of the energy fluxes in the layers of the system. The net water flux to the upper boundary surface of the system is taken as the difference of precipitation minus the evapotranspiration computed from Eq. 1.

Sensible and latent heat fluxes at the upper boundary are determined by the gradient of air temperature and moisture content between the upper boundary surface and atmosphere (Flerchinger and Saxton 1989; Flerchinger et al. 1998), which may be written as

$$H = -\rho_a c_a \frac{(T - T_a)}{r_H}, \quad (2)$$

where ρ_a, c_a and T_a are the density (kg m^{-3}), specific heat (J kg^{-1} °C^{-1}), and temperature (°C) of air at the measurement reference height, Z_{ref}; T is the temperature (°C) of the exchange surface; and r_H is the resistance to surface heat transfer (s m^{-1}), corrected for atmospheric stability.

$$E = \frac{(\rho_{vs} - \rho_{va})}{r_v}, \quad (3)$$

where ρ_{vs} and ρ_{va} are vapor density (kg m^{-3}) of the exchange surface and at the reference height, Z_{ref}; and the resistance value for vapor transfer, r_v, is taken to be equal to r_H. The resistance to convective heat transfer, r_H, is computed from

$$r_H = \frac{1}{u_* k}\left[\ln\left(\frac{z_{ref} - d + z_H}{z_H}\right) + \psi_H\right], \quad (4)$$

where u_* is the friction velocity (m s^{-1}), computed from:

$$u_* = uk\left[\ln\left(\frac{z_{ref} - d + z_m}{z_m}\right) + \psi_m\right]^{-1}, \quad (5)$$

where k is von Karman's constant, d is the zero plane displacement, z_H and z_m are the surface roughness parameters for the temperature and momentum profiles, and ψ_H and ψ_m are the diabatic correction factors for heat and momentum, computed as a function of atmospheric stability, s.

$$s = \frac{kz_{ref}gH}{\rho_a c_a T u_*^3}, \quad (6)$$

where g is gravitational acceleration. Under stable conditions ($s > 0$), $\psi_H - \psi_m = 4.7s$; under unstable conditions ($s < 0$), $\psi_m = 0.6\psi_H$

$$\psi_H = -2\ln\left(\frac{1 + \sqrt{1 - 16s}}{2}\right). \quad (7)$$

If a plant canopy is present, the surface roughness parameter for the momentum profile, z_m, is taken as 0.13 times the plant canopy height and the zero plane displacement, d, is 0.77 times the canopy height. Otherwise, the user-supplied value for z_m is used and d is set to zero. The surface roughness parameter for the temperature profile, z_H, is assumed to be $0.2z_m$.

The input parameters of the SHAW model include the initial states of snow, soil temperature, and total soil water content; diurnal or hourly weather conditions; general information about the simulation site; and parameters describing vegetation cover, snow, the residue layer, and soil. The SHAW model requires flexible parameter settings. Water and heat conditions at the lower boundary, as well as hydraulic parameters, may either be calculated or

prescribed. In this study, water and heat conditions at the lower boundary were provided by observations. Hydraulic parameters are automatically calculated by the model, and the in situ elements marked with asterisks in Table 1 during the period August 1 2002–August 31 2003 were used as forcing data. The soil was divided into 12 layers, and the soil texture of each sub-layer was obtained from Luo et al. (2008). The fraction of the surface covered by the plant canopy was 0.45 (Gao et al. 2004).

Results and discussion

Validation of the model

The SHAW model was validated by assessing the level of agreement between the measured and simulated net radiation flux, sensible heat flux, and latent heat flux. When total radiation was inputted into the model, the energy and water transmission processes were simulated within the soil–vegetation–atmosphere transfer system, and then the net radiation was simulated at the upper boundary of the system. Thus, a comparison with the measured net radiation could provide a basis for the judgment of the reliability of the simulation. Figure 2a, b shows that the simulated net radiation fitted well with the measured data for the period from August 1 2002 to August 31 2003. The linear correlation coefficient is 0.92 ($P < 0.01$, $n = 396$), with a mean bias of 9 W m^{-2}. Radiation is the main energy source of the soil–vegetation–atmosphere transfer system. Therefore, the SHAW model was found to be suitable for the simulation at the BJ site over the central Tibetan Plateau.

In addition, simulated hourly sensible and latent heat fluxes were compared with direct measurements for the periods August 1–7 2002 (Fig. 2c–f), November 27–December 18 2002 (Figs. 3a, 4a), and May 28–Jun 20

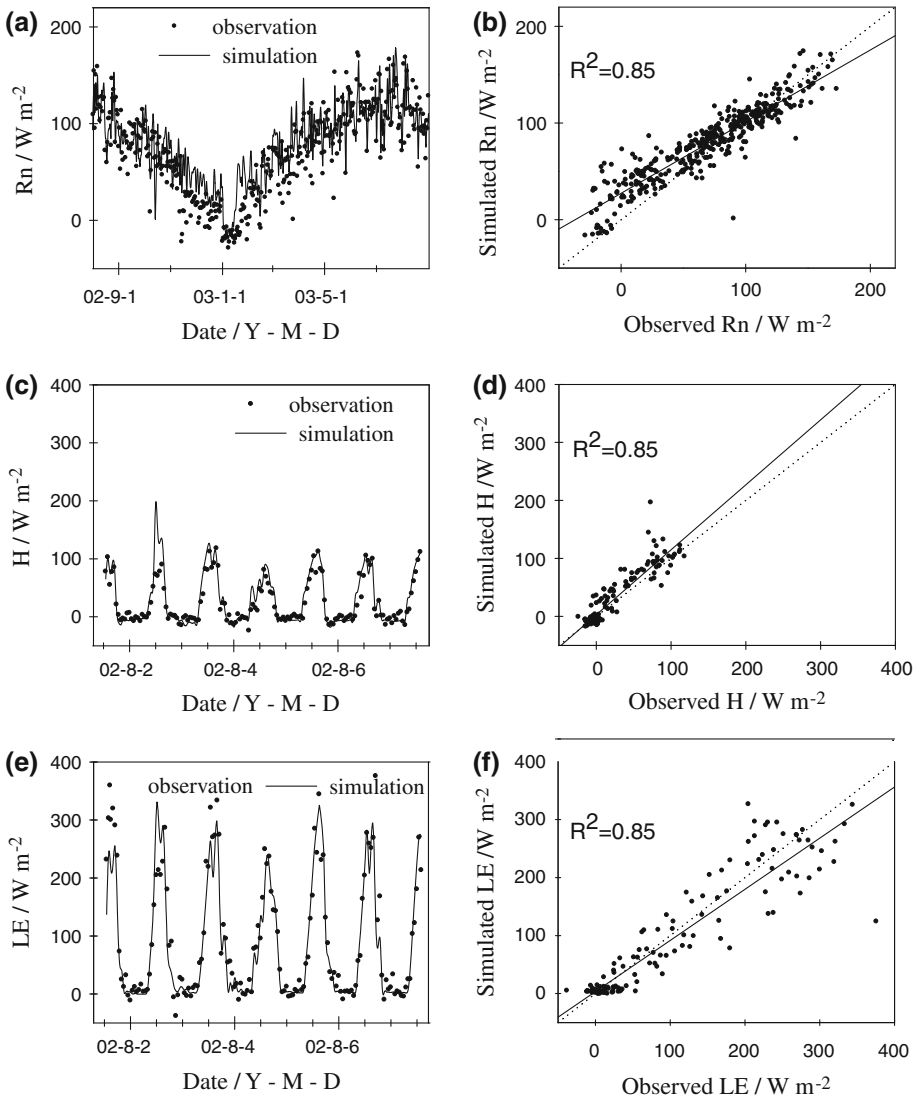

Fig. 2 Comparison of simulated and observed daily net radiation (R_n) (**a**, **b**), hourly sensible heat flux (H) (**c**, **d**) and latent heat flux (LE) (**e**, **f**). *Dotted line* represents $x = y$, and *solid line* represents the regression line

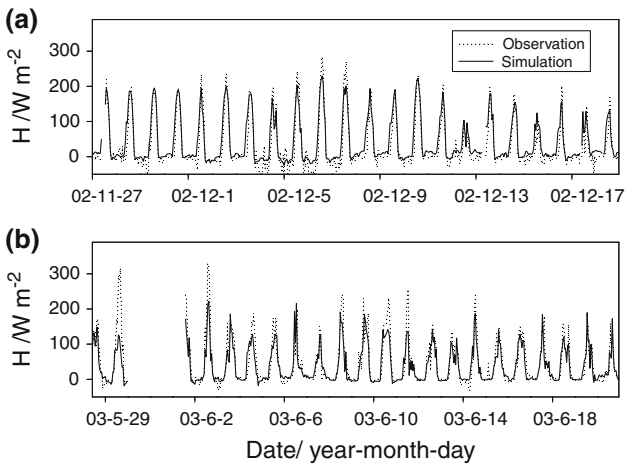

Fig. 3 Comparison of simulated and observed hourly sensible heat flux (*H*) during the period November 27 2002–December 18 2002 (**a**) and May 28 2003–June 20 2003 (**b**)

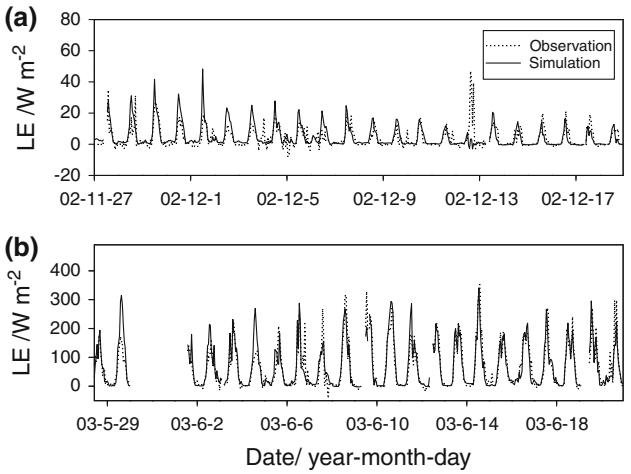

Fig. 4 Same as in Fig. 2, but for latent heat flux (*LE*)

2003 (Figs. 3b, 4b). The simulated sensible and latent heat fluxes were in close agreement with measured results during the May 28th 2003–June 20th 2003, apart from the model underestimated the diurnal maximum sensible heat flux on May 29th 2003 and June 2nd 2003, and overestimated the diurnal maximum latent flux on May 29th 2003 and June 4th 2003. Their linear correlation coefficients are 0.89 and 0.9 ($P < 0.01$, $n = 505$), with mean biases of -7.3 and 2 W m^{-2}, respectively. Also, it is apparent that the simulated sensible and latent heat fluxes yielded a good fit to observed results during the period August 1 2002 to August 7 2002. Their linear correlation coefficients are both 0.92 ($P < 0.01$, $n = 146$), with mean biases of 5.8 W m^{-2} and -7.6 W m^{-2}, respectively. During the period between November 27 2002 and December 18 2002, the simulated sensible heat flux can be seen to fit closely with measured results, with a linear correlation coefficient of 0.93 ($P < 0.01$, $n = 521$) and mean bias of 13 W m^{-2}. The simulated latent heat flux also shows good agreement with observed results, except on December 12. Moreover, the model overestimated the maximum latent heat flux on December 1 and 2. Their linear correlation coefficients are 0.66 ($P < 0.01$, $n = 521$), with mean biases of 0.7 W m^{-2}. Thus, it was found that the SHAW model can reasonably simulate the sensible and latent heat flux at the BJ site on the central Tibetan Plateau.

Response of sensible and latent heat flux to the diurnal range of soil surface temperature and moisture

Figure 5 shows soil temperature changes at a depth of 2 cm and the diurnal range of unfrozen water content, sensible heat flux, and latent heat flux. The yellow band denotes the freezing stage, the green band denotes the thawing stage, the area between the two bands denotes the completely frozen stage, and the outside of them denotes the completely thawed stage. Yang et al. (2007) examined the days of the four freeze/thaw stages and found that the time that the surface undergoes diurnal freeze/thaw cycles is approximately 6 months. In this study, an attempt was made to investigate the relationship between sensible and latent heat flux and diurnal variation in soil surface temperature and moisture under four soil freeze/thaw conditions.

Rain can influence sensible and latent heat flux through indirectly increasing soil water content. However, snow can directly influence sensible and latent heat flux through evaporation of snowmelt water or snow sublimation. In order to remove the impact of snow on sensible and latent heat flux, snowfall was not considered when running the model. Figure 5g, h shows the diurnal range of the simulated, sensible, and latent heat flux, without consideration of the impact of snow.

During the completely thawed stage, soil temperature at a depth of 2 cm is >0°C. Soil water content is sufficient during both the daytime and at night due to high levels of precipitation, which results in a quite weak diurnal range. The diurnal range of latent heat flux is significant, which is due to evaporation-generated latent heat being larger during the daytime, but smaller at night because of no heating by solar radiation. Although heating by solar radiation is strong during the daytime, the sensible heat flux is still small, which results from the absorbing of heat from the evaporation of soil surface water. Additionally, the sensible heat flux is also small at night, hence leading to a relatively low diurnal range.

During the completely frozen stage, the daily maximum temperature decreases evidently, and it is interesting that an obvious increase in the daily minimum temperature can be seen. The diurnal range of the latent heat flux reaches its

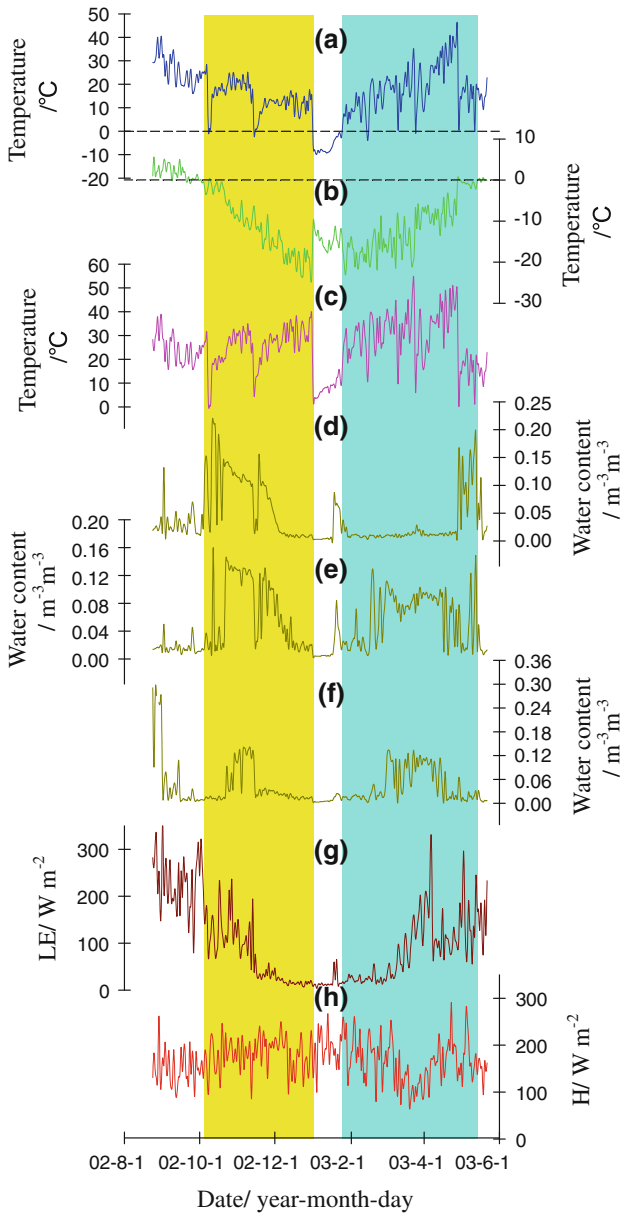

Fig. 5 Diurnal maximum soil temperature (**a**), diurnal minimum soil temperature (**b**), diurnal range of soil temperature (**c**), at a depth of 2 cm; diurnal range of soil unfrozen water content at 0–3 cm (**d**), 3–6 cm (**e**), and 18.5–21.5 cm (**f**), and diurnal range of latent heat flux (*LE*) (**g**) and sensible heat flux (*H*) (**h**)

lowest level of the year, and this is due to the quite low diurnal range of unfrozen soil water content. The sensible heat flux is relatively high because solar radiation is mainly allocated to it.

During the freezing stage, the diurnal range of soil temperature is significant. The diurnal range of unfrozen soil water content at depths of 0–3 cm and 3–6 cm are larger than that at depths of 18.5–21.5 cm. This indicates that frequent soil water phase transition, caused by the diurnal freeze/thaw cycle, occurs mainly at the interface (i.e. ground surface). The diurnal range of the latent heat flux is significant during the period October 9–November 1. The diurnal range of the unfrozen soil water content at depths of 0–3 cm is also significant during this period. The diurnal ranges of latent heat flux decrease sharply on October 8, 14, and 19, and the diurnal range of the unfrozen soil water content at depths of 0–3 cm also decreases sharply on these days. This indicates a good relationship between the diurnal ranges of latent heat flux and unfrozen soil surface water content. The diurnal range of the sensible heat flux is low during this period, the reason for which is similar to that of the completely thawed stage.

The thawing stage is 20 days longer than the freezing stage at a depth of 2 cm. The diurnal ranges of unfrozen soil water content at depths of 3–6 cm and 18.5–21.5 cm during the thawing stage are similar to those during the freezing stage. However, the diurnal range of unfrozen soil water content at depths of 0–3 cm during the thawing stage is much lower than during the freezing stage, which results from the very low total soil water content (unfrozen water and ice). The low total soil water content is caused by two factors: (1) the surface frozen soil undergoes sublimation for approximately one month (the completely frozen stage); and (2) precipitation is very low in winter. If the surface soil is dry, evaporation will occur in lower layers according to the function of the soil water potential gradient (Kondo and Saigusa 1994; Kondo and Xu 1997; Xu and Haginaya 2001). Therefore, latent heat flux change during the thawing stage is mainly caused by the evaporation of unfrozen soil water content at depths of 3–6 cm. The diurnal range of latent heat flux is significant during the period March 8–April 6, and the diurnal range of unfrozen soil water content at depths of 3–6 cm is also significant during the period February 28–April 16. This indicates that there is a better relationship between the diurnal ranges of both latent heat flux and unfrozen soil water content. In addition, the period that the diurnal range of the unfrozen soil water content is significant is longer than that of latent heat flux. This demonstrates the impact of other factors (e.g. solar radiation and wind speed) on latent heat flux.

The sensible heat flux is large during the period January 25–March 5 due to a dry ground surface, but decreases during the period March 6–April 6. In contrast, latent heat flux increases during this period, but decreases during the period April 6–April 28, while sensible heat flux increases. This indicates an anti-correlation relationship between these two elements. Further, the latent heat flux increases again during the period April 28–May 14, while the sensible heat flux again decreases due to increasing precipitation. After May 14, soil at a depth of 2 cm begins the completely thawed stage again.

Response of sensible and latent heat flux to diurnal variation in soil surface soil temperature and moisture

In order to remove the impact of changes in extreme weather elements on sensible and latent heat flux, two continuous clear days from each freeze/thaw stage were chosen as a case study. September 8 and 9 denote the completely thawed stage, October 29 and 30 the freezing stage, January 10 and 11 the completely frozen stage and March 28 and 29 the thawing stage. Additionally, in order to remove the impact on sensible and latent heat flux of differences in wind speed for the four freeze/thaw stages, the wind speed of the chosen day was adjusted to equivalence before running the model.

The diurnal mean soil temperatures during the different freeze/thaw stages are different (Table 3), and the diurnal variations in soil temperature are negligible during the completely frozen stage. Diurnal variations in soil temperature at a depth of 2 cm are more significant than at 5 and 20 cm, and diurnal variations in soil temperature during the freezing stage are similar to those during the thawing stage (Fig. 6).

Diurnal variation in soil temperature is significant during the completely thawed stage, while diurnal variation of unfrozen soil water content is negligible, which indicates a weak relationship between them during this period. There is almost no diurnal variation in unfrozen soil water content during the completely frozen stage (Fig. 6); however, they are quite significant during the freezing and thawing stages, which indicates that the diurnal freeze/thaw cycles result in diurnal cycles of soil water phase change. The diurnal variation pattern of unfrozen soil water content during the freezing stage is similar to that during the thawing stage. However, the diurnal range of unfrozen soil water content during the thawing stage is slightly weaker than during the freezing stage (Table 4). In particular, unfrozen soil water content at depths of 0–3 cm shows almost no diurnal variation, which is due to lower total soil water content during the thawing stage than the freezing stage.

Diurnal variations in both latent heat flux and solar radiation are significant during the completely thawed stage, but that of soil water content is negligible. Under sufficient soil water content in this stage, latent heat flux is larger during the daytime due to higher air temperatures from strong solar radiation, but smaller at night because of no solar radiation. Thus, diurnal variation in latent heat flux depends mostly on solar radiation during the completely thawed stage. Diurnal variation in latent heat flux is quite weak during the completely frozen stage due to relatively low unfrozen soil water content; however, it still exists because of the effect of salinity on the freezing point of soil. Meanwhile, diurnal variation in solar radiation is significant (Fig. 6), and hence diurnal variation in latent heat flux depends mostly on the unfrozen soil water content during the completely frozen stage.

Diurnal variation in latent heat flux is significant during the freezing and thawing stages because diurnal variations in both unfrozen soil water content and solar radiation are significant. Diurnal variation in unfrozen soil water content during the thawing stage is smaller than during the freezing stage (Table 5); however, the latent heat flux during the thawing stage is larger than during the freezing stage due to stronger solar radiation during the former stage (Fig. 6). Strong solar radiation can influence evaporation-generated latent heat flux through increasing air temperature. Thus, during the freezing and thawing stages diurnal variation in the latent heat flux depends mostly on diurnal variation in soil moisture. However, the impact of changes in air temperature due to solar radiation cannot be ignored.

Diurnal variations in the sensible heat flux are significant during the four soil freeze/thaw stages. Sensible heat flux is relatively small during the completely thawed stage due to high levels of precipitation, with solar radiation mainly allocated to latent heat flux. However, sensible heat flux is relatively large during the completely frozen stage due to dry ground, with solar radiation mainly allocated to it. The daily mean sensible heat flux during the freezing and thawing stages lies between the completely frozen stage and the completely thawed stage (Table 6).

Concluding remarks

The diurnal ranges of both unfrozen soil water content and sensible heat flux were found to be relatively low during the completely thawed stage; however, the diurnal range of

Table 3 Statistics of diurnal variation in soil temperature at a depth of 2 cm during the four soil freeze/thaw stages (°C)

Date/month-day	Completely thawed stage		Freezing stage		Completely frozen stage		Thawing stage	
	09-08	09-09	10-29	10-30	01-10	01-11	03-28	03-29
Maximum	28.9	32.4	22.9	17.5	−8.6	−8.8	25.6	28.5
Minimum	1.2	0	−9.1	−9.0	−16.4	−17.0	−10.5	−11.7
Daily range	27.7	32.4	32.0	26.5	7.8	8.2	36.1	40.2
Daily mean	11.6	9.9	1.6	0.7	−13.2	−13.6	1.7	3.1

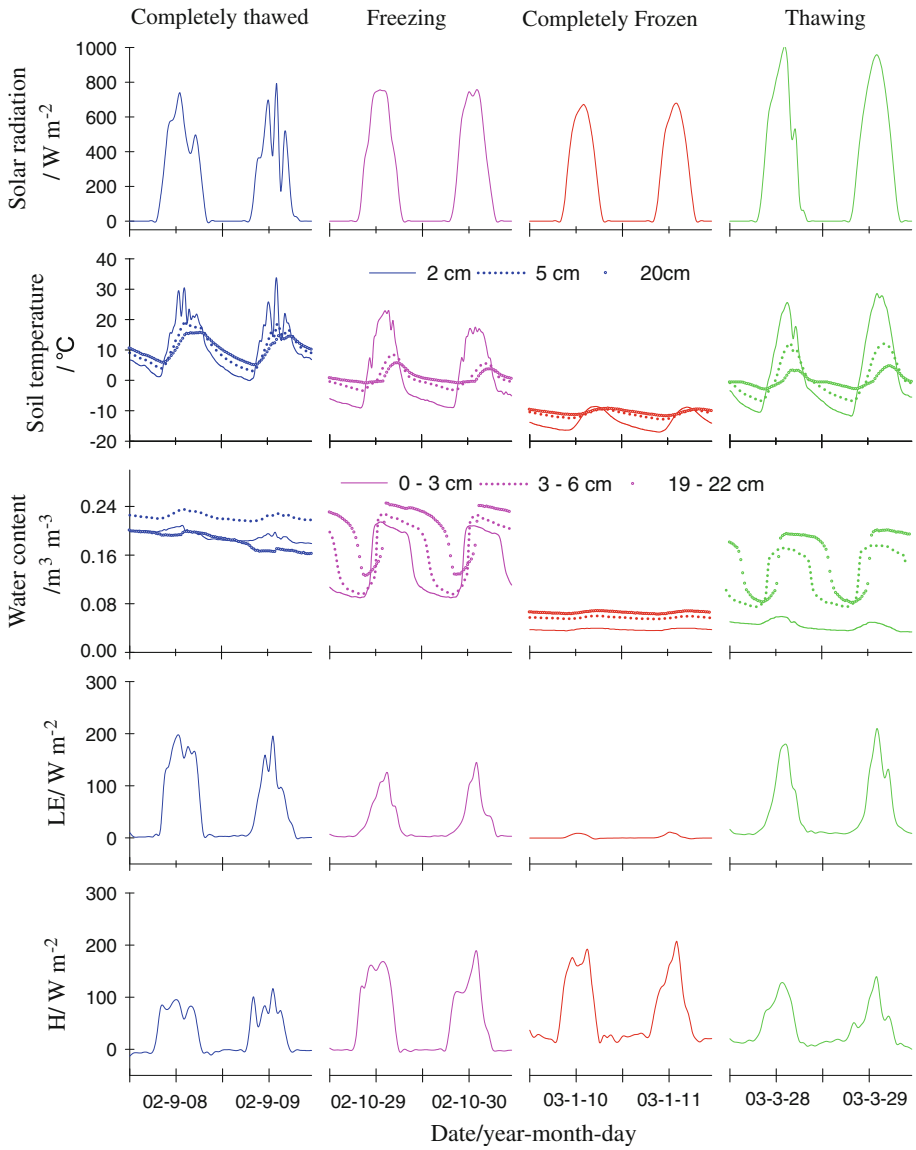

Fig. 6 Diurnal variation in solar radiation, soil temperature, unfrozen soil water content, latent heat flux (*LE*), and sensible heat flux (*H*) during the four freeze/thaw stages

Table 4 Same as in Table 3, but for unfrozen soil water content at 0–3 cm (m^3 m^{-3})

Date/month-day	Completely thawed stage		Freezing stage		Completely frozen stage		Thawing stage	
	09-08	09-09	10-29	10-30	01-10	01-11	03-28	03-29
Maximum	0.208	0.198	0.214	0.208	0.040	0.040	0.172	0.176
Minimum	0.185	0.179	0.090	0.090	0.035	0.036	0.075	0.075
Daily range	0.023	0.019	0.124	0.118	0.005	0.004	0.097	0.101
Daily mean	0.198	0.186	0.145	0.144	0.038	0.038	0.123	0.128

latent heat flux was relatively large during this stage. During the completely frozen stage, the diurnal ranges of both unfrozen soil water content and latent heat flux were found to be quite weak; however, the diurnal range of sensible heat flux was relatively large. The diurnal ranges of both latent heat flux and unfrozen soil water content at depths of 0–3 cm were found to have similar patterns of temporal change during the freezing stage, indicating a good relationship between them. During the thawing stage, the diurnal range of latent heat flux was found to relate to that of unfrozen soil water content at depths of 3–6 cm. Furthermore, the diurnal range of latent heat flux showed an anti-correlation relationship with that of sensible heat flux.

Table 5 Same as in Table 3, but for latent heat flux (W m^{-2})

Date/month-day	Completely thawed stage		Freezing stage		Completely frozen stage		Thawing stage	
	09-08	09-09	10-29	10-30	01-10	01-11	03-28	03-29
Maximum	193	196	123	144	8	11	178	210
Minimum	2	0	2	2	−3	−3	6	8
Daily range	191	196	121	142	11	12	172	202
Daily mean	67	45	32	30	1	1	48	53

Table 6 Same as in Table 3, but for sensible heat flux (W m^{-2})

Date/month-day	Completely thawed stage		Freezing stage		Completely frozen stage		Thawing stage	
	09-08	09-09	10-29	10-30	01-10	01-11	03-28	03-29
Maximum	95	116	168	188	191	207	126	138
Minimum	−13	−6	−4	−3	13	14	6	0
Daily range	108	122	172	191	178	193	120	138
Daily mean	31	29	56	48	72	67	43	41

Diurnal variation in latent heat flux was found to depend mostly on solar radiation during the completely thawed stage. Diurnal variation in latent heat flux was quite weak during the completely frozen stage due to low unfrozen soil water content, while diurnal variation in solar radiation was found to be significant. Thus, diurnal variation in latent heat flux depended mostly on unfrozen soil water content during this stage. During the freezing and thawing stages, diurnal variation in latent heat flux was found to be significant, dependent mostly on diurnal variation in unfrozen soil water content. However, the impact of changes in air temperature due to solar radiation could not be ignored.

Ground surface soil undergoes diurnal freeze/thaw cycles. Diurnal variation in soil temperature results in diurnal variation in unfrozen soil water content, which in turn affects sensible and latent heat fluxes. However, sensible and latent heat fluxes are not only influenced by unfrozen soil water content, but also by changes in the weather (e.g. snowfall and wind speed). This makes it difficult to research solely the impact of soil temperature and moisture on sensible and latent heat flux, eliminating the complex impact of the weather. In this study, the impacts of snow and wind speed difference were removed. Further exclusion of other weather-related impacts, in order to study quantitatively the relationship between land surface heat flux and soil temperature and moisture, is something worthy of future examination. In addition, although the SHAW model was validated to be applicable for ground surface heat and water transfer on the Tibetan Plateau, the simulated sensible and latent heat fluxes might to some extent have still caused biases. Therefore, detailed long-term observations of sensible and latent heat fluxes are required in future so as to achieve a more accurate examination.

Acknowledgments This research was sponsored jointly by the National Key Basic Research program of China (2010CB951404), the One Hundred Talent Program of the Chinese Academy of Sciences (29O827B11), the Key International Cooperation Project of NSFC (40810059006), and the National Key Basic Research Program of China (2009CB421406). Sensible and latent heat flux data were provided by NCAR/EOL under sponsorship of the National Science Foundation. Opinions, findings, conclusions, and recommendations expressed in this paper are those of the authors and do not necessarily reflect the views of the National Science Foundation. We are indebted to the reviewers for helpful comments and criticisms of the initial draft of this paper.

References

Cheng HY, Wang GX, Hu HC, Yang YB (2008) The variation of soil temperature and water content of seasonal frozen soil with different vegetation coverage in the headwater region of the Yellow River, China. Environ Geol 54:1755–1762

Duan AM, Wu GX (2005) Role of the Tibetan Plateau thermal forcing in the summer climate patterns over subtropical Asia. Clim Dyn 24:793–807

Flerchinger BN, Pierson FB (1991) Modeling plant canopy effects on variability of soil temperature and water. Agric For Meteorol 56:227–246

Flerchinger BN, Saxton KE (1989) Simultaneous heat and water model of a freezing snow-residue-soil system, I, theory and development. Trans ASAE 32:567–571

Flerchinger GN, Hanson CL, Wight JR (1996) Modeling evapotranspiration and surface energy budgets across a watershed. Water Resour Res 32:2539–2548

Flerchinger BN, Kustas WP, Weltz MA (1998) Simulating surface energy and radiometric surface temperatures for two arid vegetation communities using the SHAW model. J Appl Meteorol 37:449–460

Gao ZQ, Chae N, Kim J, Hong J, Choi T, Lee H (2004) Modeling of surface energy partitioning, surface temperature and soil wetness in the Tibetan prairie using the simple biosphere model 2(SiB2). J Geophys Res 109:D06102. doi:10.1029/2003JD004089

Guo DL, Yang MX, Li M, Qu P (2009a) Analysis on simulation of characteristic of land surface energy flux in seasonal frozen soil region of central Tibetan Plateau. Plateau Meteorol 28:978–987 (in Chinese with English Abstract)

Guo DL, Yang MX, Qu P, Wan GN, Wang XJ (2009b) Studies of the energy and water cycle processes: review and discussion. J Glaciol Geocryol 31:1116–1126 (in Chinese with English Abstract)

Kondo J, Saigusa N (1994) Modelling the evaporation with a formula for vaporization in the soil pores. J Meteorol Soc Jpn 72:413–421

Kondo J, Xu J (1997) Seasonal variations in the heat and water balances for nonvegetated surfaces. J Appl Meteorol 36:1676–1695

Li SX, Nan ZT, Zhao L (2002) Impact of soil freezing and thawing process on thermal exchange between atmosphere and ground surface. J Glaciol Geocryol 24:506–511 (in Chinese with English Abstract)

Luo SQ, Lv SH, Zhang Y, Hu ZY, Ma YM, Li SS, Shang LY (2008) Simulation analysis on land surface process of BJ site of central Tibetan Plateau Using CoLM. Plateau Meteorol 27:259–271 (in Chinese with English Abstract)

Ma WQ, Ma YM (2006) The annual variations on land surface energy in the northern Tibetan Plateau. Environ Geol 50:645–650

Ma YM, Fan S, Ishikawa H, Tsukamoto O, Yao T, Koike T, Zuo H, Hu Z, Su Z (2004) Diurnal and inter-monthly variation of land surface heat fluxes over the central Tibetan Plateau area. Theor Appl Climatol 80:259–273

Ma WQ, Ma YM, Li MS, Su Z, Wang JM (2005) Seasonal variation on land surface energy budget and energy balance components in the Northern Tibetan Plateau. J Glaciol Geocryol 27:673–679 (in Chinese with English Abstract)

Ma YM, Yao TD, Wang JM (2006) Experimental study of energy and water cycle in Tibetan Plateau-the progress introduction on the study of GAME/Tibet and CAMP/Tibet. Plateau Meteorol 25:344–351 (in Chinese with English Abstract)

Tanaka K, Ishikawa H, Hayashi H, Tamagama I, Ma YM (2001) Surface energy budget at Amdo on theTibetan Plateau using GAME/Tibet IOP 98 data. J Meteorol Soc Jpn 79:505–517

Ueda H, Yasunari T (1998) Role of warming over the Tibetan Plateau in early onset of the summer monsoon over the bay of bengal and the South China Sea. J Meteorol Soc Jpn 76:13–27

Webster PJ (1987) In: Fein JS, Stephens PL (eds) Monsoons, Wiley, New York, pp 3–32

Wu GX, Chen SJ (1985) The effect of mechanical forcing on the formation of a mesoscale vortex. Q J Royal Meteorol Soc 111:1049–1070

Wu GX, Zhang YS (1998) Tibetan Plateau forcing and the timing of the monsoon onset over south Asia and the Southern China Sea. Mon Weather Rev 126:913–927

Xu J, Haginaya S (2001) An estimation of heat and water balances in the Tibetan Plateau. J Meteorol Soc Jpn 79:485–504

Yanai MH, Li CF, Song ZS (1992) Seasonal heating of the Tibetan Plateau and its effects on the evolution of the Asian summer monsoon. J Meteorol Soc Jpn 70:319–351

Yang MX, Yao TD, Ding YJ, Wang SL, Chen XZ, Toshio K, Takeo T (1999a) The diurnal variation of the soil temperature in the Northern Tibetan Plateau. Environ Sci 20:5–8 (in Chinese with English Abstract)

Yang MX, Yao TD, Wang SL, Ding YJ, Chen XZ, Shen YP, Toshio K (1999b) The features of soil temperature and moisture on Northern Tibetan Plateau. Geogr Res 18:313–317 (in Chinese with English Abstract)

Yang MX, Yao TD, Gou XH (2003) The soil moisture distribution, thawing-freezing processes and their effects on the seasonal transition on the Qinghai-Xizang(Tibetan) plateau. J Asian Earth Sci 21:457–465

Yang MX, Yao TD, Gou XH, Hirose N, Fujii HY, Hao LS, Levia DF (2007) Diurnal freeze/thaw cycles of the ground surface on the Tibetan Plateau. Chin Sci Bull 52:136–139

Ye DZ, Gao YX (1979) Meteorology of the Tibetan Plateau. Science Press, Beijing, pp 30–55

Yu JH, Liu JM, Ding YG (2004) Annual and diurnal variation of surface fluxes in Western Qinghai-Xizang Plateau. Plateau Meteorol 23:354–359 (in Chinese with English Abstract)

Zhao YZ, Ma YM, Ma WQ, Li MS, Sun FL, Wang L, Xiang M (2007) Variation of soil temperature and soil moisture in Northern Tibetan Plateau. J Glaciol Geocryol 29:578–583 (in Chinese with English Abstract)